

# Characterization and Crystallization Kinetics of a Diopside-Based Glass-Ceramic Developed from Glass Industry Raw Materials

M. L. Öveçoğlu,<sup>a</sup> B. Kuban<sup>b</sup> & H. Özer<sup>a</sup>

<sup>a</sup>Department of Metallurgical Engineering, Faculty of Chemistry-Metallurgy, Istanbul Technical University, Maslak 80626, Istanbul/Turkey

<sup>b</sup>Business Development, ŞİŞECAM, Camhan, Barbaros Bul. 125, Beşiktaş, Istanbul 80706, Turkey

(Received 23 October 1995; revised version received 12 September 1996; accepted 23 September 1996)

## Abstract

Glass industry raw materials blended with 10 wt% technical grade  $TiO_2$  powders were used to develop a glass-ceramic of the  $SiO_2$ - $MgO$ - $Al_2O_3$ - $CaO$ - $(Na_2O, K_2O)$  system. On the basis of the DTA analysis, nucleation and crystallization experiments were carried out at 735 and 870°C, respectively. X-ray diffraction studies performed on the glass-ceramic system revealed the presence of the diopside as the major crystallizing phase comprising about 74 vol%. SEM investigations showed that the diopside crystals were formed as a result of surface nucleation and were conical in shape, between 15 and 40  $\mu m$  in length and between 5 and 13  $\mu m$  in width. DTA analyses were conducted at different heating rates and an activation energy for surface crystallization value of 150 kJ/mole was determined graphically from a Kissinger-type plot using the analysis of Matusita and Sakka. This value is about half of that for the same glass composition without the  $TiO_2$  content. © 1997 Elsevier Science Limited.

## 1 Introduction

Research and development investigations pertaining to glass-ceramic materials have been underway for more than three decades.<sup>1–20</sup> Since glass is the starting material for glass-ceramics, the glass industry plays a central role in the search for potential compositions which can be exploited for glass-ceramics development. In other words, cheap and abundant raw materials constituting commercial glass batch compositions can be modified to achieve the kinetically most advantageous formulation within the phase separating fields of the  $SiO_2$ - $MgO$ - $Al_2O_3$ - $CaO$  quaternary system. Earlier research work in this quaternary system with

substantial nucleant additions (5–10 wt%) reported the formation of cordierite ( $Al_4Mg_2Si_5O_{18}$ ) as the primary crystallizing phase in some of the resultant glass-ceramic materials,<sup>4,8–12,17</sup> while quartz,<sup>8,16,17</sup> akermanite ( $Ca_2MgSi_2O_7$ )<sup>14</sup> and gehlenite ( $Ca_2Al_2Si_2O_7$ )<sup>14</sup> were present in others. However, it is interesting to note that industrial grade glass-forming raw materials were not utilized in these investigations; either technical grade powders<sup>8,12–17</sup> or glass plates<sup>9–12</sup> were used as the starting materials. The development of glass-ceramics from industrial grade raw materials or waste materials containing diopside or pyroxene type phases has been accomplished in the last 15 years.<sup>18–20</sup>

In an effort to scale up laboratory results to pilot-scale production level in conventional glass melting and casting routes, a recent study carried out on various glass compositions and nucleating agents such as chromite and magnetite has demonstrated that raw materials for glass can be used in glass-ceramic production without the need of concentration and purification.<sup>21</sup> The resultant glass-ceramics were diopside-based and possessed properties which qualified them as candidates for construction purposes.<sup>21,22</sup> Differential thermal analysis (DTA) techniques were used to determine the glass transition ( $T_g$ ) and the crystallization ( $T_c$ ) temperatures for the optimization of the proportions of nucleating agents and crystallization temperatures for that study.<sup>21–23</sup> The DTA technique has been widely accepted and used by a number of researchers as a rapid and convenient analytical tool in investigating the kinetics of chemical reactions and crystallization of glasses.<sup>24–29</sup> As reported by some of these investigators, the activation energy for crystal growth within a surrounding parent glass can be estimated from the DTA curves scanned at different heating rates by

analysing the exothermic crystallization peak height on the basis of classical nucleation and crystallization theory.<sup>25,26</sup> The prerequisite for such DTA analyses is the microstructural characterization of the predominant crystallization mechanism, viz. whether the crystallization takes place by bulk or surface nucleation, in order to determine the activation energy for crystallization.<sup>28</sup>

The present study investigates the crystallization kinetics and characterization of a glass-ceramic material based on a chemical composition selected during the earlier above-mentioned optimization studies of several compositions in the  $\text{SiO}_2$ - $\text{MgO}$ - $\text{Al}_2\text{O}_3$ - $\text{CaO}$ - $(\text{Na}_2\text{O}, \text{K}_2\text{O})$  system.<sup>21-23</sup> Glass industry raw materials and technical grade titania powders were used respectively to form the parent glass and the resultant glass-ceramic material containing diopside as the crystallizing phase detected by X-ray diffractometry techniques. DTA techniques were employed to determine the glass transition ( $T_g$ ) and peak crystallization ( $T_p$ ) temperatures at different heating rates from which the activation energy for surface crystallization of the diopside crystals in the parent glass matrix was estimated. The morphologies of diopside crystals in the glass-ceramic were characterized by using scanning electron microscopy (SEM) techniques.

## 2 Experimental Procedure

The main glass industry raw materials, quartz, dolomite, limestone and fluorospar, were blended in various proportions to constitute the following chemical composition of the parent glass (in wt%): 50  $\text{SiO}_2$ , 20  $\text{CaO}$ , 10  $\text{MgO}$ , 10  $\text{Al}_2\text{O}_3$  and 10 alkali oxide (all compositions in this study are given in wt%, unless otherwise stated). After drying and pulverizing steps, technical grade  $\text{TiO}_2$  powders were added as 10% of the total batch followed by grinding in a conventional ceramic ball mill for about 10 h. Melting was performed in Pt crucibles at 1450°C for about 6 h followed by casting onto stainless steel moulds at room temperature. Immediately following the casting procedure, the glass samples were removed from the moulds, placed in a furnace and annealed at 500°C for 1 h.

Differential thermal analysis (DTA) scans of annealed glass specimens were carried out either in a Rigaku Thermoflex apparatus or in a Perkin-Elmer 7 Series Thermal Analyzer in order to determine the characteristic glass transition temperatures,  $T_g$ , and peak crystallization temperatures,  $T_p$ . After pulverizing and grinding as-cast glass to a size of about 30  $\mu\text{m}$ , static non-isother-

mal experiments were performed by heat treating 100 mg glass powder in a platinum crucible and using the same amount of  $\text{Al}_2\text{O}_3$  as the reference in a temperature range between 25°C and 1200°C at heating rates of 5, 10, 15, 20 and 25°C/min. Data for each run were collected directly from the DTA. Nucleation and crystallization experiments of annealed glass samples were performed in a muffle furnace which had an approximate optimum heating rate of 6°C/min. For this reason, the data of the DTA curve given in Fig. 1 for the heating rate of 5°C/min were chosen as the reference for the nucleation and crystallization conditions of 735°C/16 h and 870°C/40 min, respectively.

Microstructural characterizations of the crystallized glass-ceramic samples were performed by using both electron microscopy and X-ray diffraction techniques. Scanning electron microscopy (SEM) investigations were conducted by using a JEOL™ 733 Electrone Superprobe operated at 25 kV and linked with an energy dispersive spectrometry (EDS) attachment. The X-ray diffraction investigations were carried out in a Siemens™ D-5000 diffractometer using  $\text{Cu } K_\alpha$  radiation at 40 kV and 30 mA settings in the  $2\theta$  range from 20° to 60° at a scanning speed of 0.03°/min. The phases were identified by comparing the peak

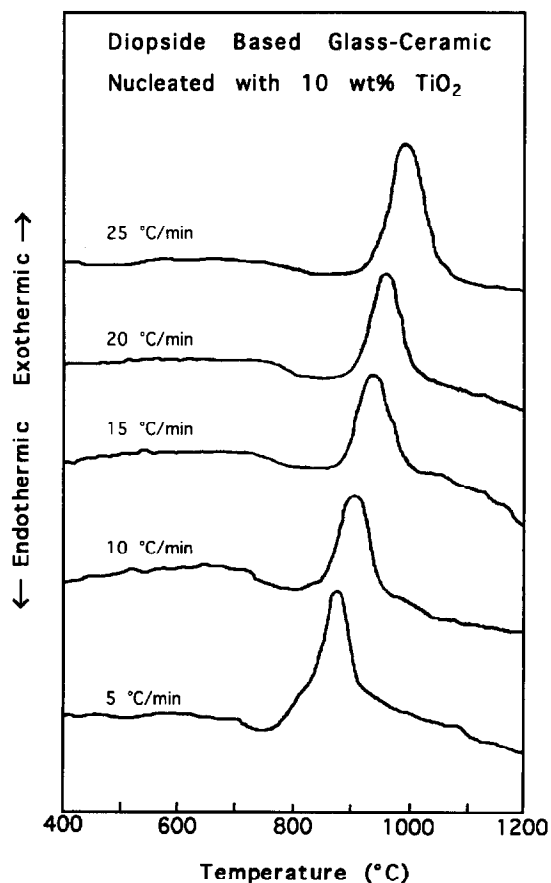


Fig. 1. Differential Thermal Analysis (DTA) curves of the 10 wt%  $\text{TiO}_2$  added diopside-based glass-ceramic scanned at heating rates of 5, 10, 15, 20 and 25°C/min.

positions and intensities with those listed in the JCPDS (Joint Committee on Powder Diffraction Standards) files. Quantitative X-ray diffractometry methods were carried out using the Siemens DIFFRAC-AT software to predict the amount of the major crystallizing phase and the amorphous glass matrix. Readily available pure diopside (99.92% purity) and titania powders (99.98% purity) were used as internal standards for the quantitative X-ray analysis.

### 3 Results and Discussion

#### 3.1 Thermal analysis

DTA investigations on the titania-containing glass were carried out to determine the nucleation and crystallization temperatures used in designing a glass-ceramic material with optimum properties. Figure 1 shows the DTA thermograms of the TiO<sub>2</sub>-containing glass scanned at heating rates of (a) 5°C/min, (b) 10°C/min, (c) 15°C/min, (d) 20°C/min, and (e) 25°C/min. Whereas the endothermic peaks detected in all scans correspond to the glass transition temperatures,  $T_g$ , the exothermic ones belong to the peak crystallization temperatures,

**Table 1.** Heating rate, glass transition and peak crystallization temperatures detected during the DTA scans

B (°C/min)	$T_g$ (°C)	$T_p$ (°C)
5	707	875
10	718	905
15	729	933
20	739	960
25	749	986

$T_p$ . The  $T_g$  and  $T_p$  values for different heating rates are listed in Table 1. As expected, both the  $T_g$  and  $T_p$  temperatures shift to higher values with increasing rate, a behaviour also reported in the DTA studies of other glass systems.<sup>25,27-30</sup> In a similar investigation where diopside was the major crystallizing phase in the ternary SiO<sub>2</sub>-CaO-MgO system, Baldi *et al.*<sup>20</sup> reported lower  $T_g$  and  $T_p$  values (687°C and 885°C, respectively) at the heating rate of 20°C/min than those found in this study. We believe that these differences can be attributed to the presence of Al<sub>2</sub>O<sub>3</sub> which was absent in that study and to the lower MgO content in our investigation. In addition, industrial grade powders possibly containing impurities and larger pulverized glass particles (~30 μm) for the DTA analyses utilized in this study contributed to these differences.

#### 3.2 Microstructural characterization

Figure 2 shows the X-ray diffraction pattern of the glass-ceramic material. As seen in Fig. 2, all the diffraction peaks can be indexed as arising from the reflection planes of the diopside-aluminan phase of the chemical formula Ca(Mg, Al)(Si, Al)<sub>2</sub>O<sub>6</sub> which has a monoclinic structure with lattice parameters  $a = 0.973$  nm,  $b = 0.887$  nm,  $c = 0.528$  nm and  $\beta = 105.92^\circ$ .<sup>31</sup> In addition, a small amount of TiO<sub>2</sub> as tetragonal rutile phase with lattice parameters  $a = 0.459$  nm and  $c = 0.296$  nm is present.<sup>32</sup> Since the crystallization takes place in the parent glass matrix, knowing the amount of the major crystallizing phase is a valid indication for the efficiency of the heat treatment cycle and the nucleant employed for the

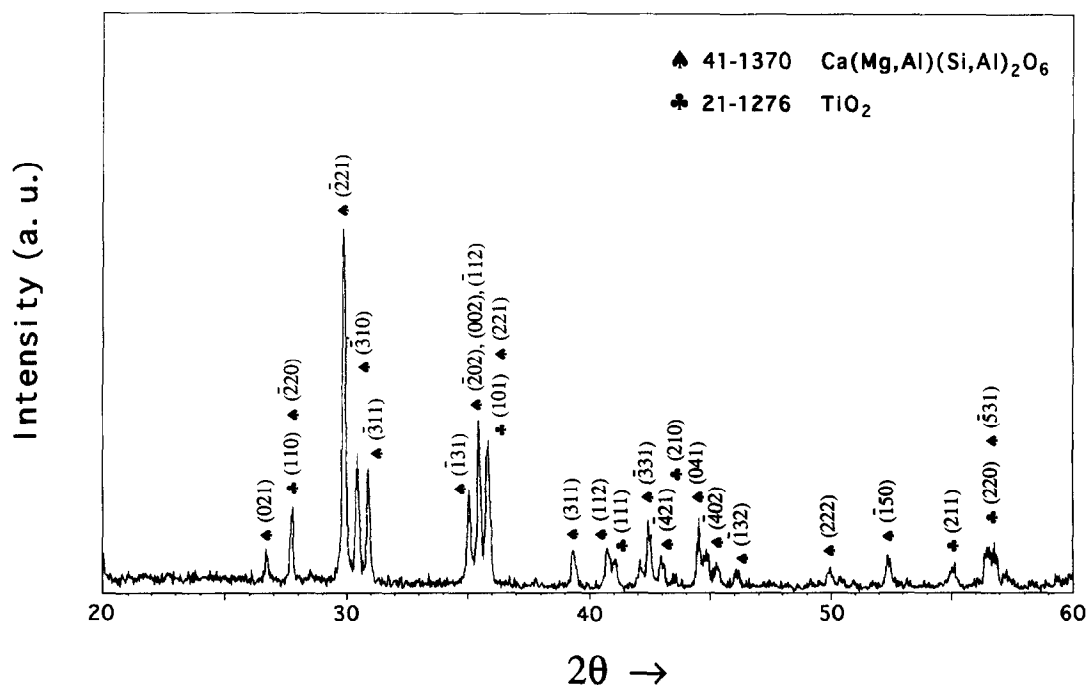


**Fig. 2.** X-ray diffraction pattern of the diopside-based glass-ceramic material scanned in the  $2\theta$  range from 20° to 60°.

starting raw material batch. For this purpose, the quantitative methods of Chung<sup>33,34</sup> were used. The amount of the major crystallizing phase  $\text{Ca}(\text{Mg},\text{Al})(\text{Si},\text{Al})_2\text{O}_6$  was determined to be about 74 vol%, that of the nucleant rutile as 7 vol% and the balance of about 19 vol% belonging to the parent glass. Similar compositional values were also obtained when the method of Ohlberg and Strickler<sup>35</sup> was used. As mentioned earlier, diopside phase crystallization in the ternary  $\text{SiO}_2$ - $\text{CaO}$ - $\text{MgO}$  system was also observed by Baldi *et al.*<sup>20</sup> who reported the starting crystallization temperature as 1000°C and complete crystallization above 1100°C.

To obtain better understanding of the morphology and size of the crystallizing phases, SEM investigations were conducted. Figures 3(a) and (b) are typical SEM micrographs of the glass-ceramic taken respectively from a crystal-rich and a glass-rich region showing conical rod-like crystals fanning out from an initial base. A qualitative EDS analysis on several crystals revealed that they



(a)



(b)

Fig. 3. Typical scanning electron micrographs taken from the glass-ceramic material showing conical shaped rod-like diopside crystals: (a) in a crystalline-rich region, (b) embedded in the glassy matrix.

contained about 8 vol% Mg, an indication that they should be diopside crystals. As seen in Fig. 3(a), the length of the crystals ranges between 15 and 40  $\mu\text{m}$  whereas their width is about 5  $\mu\text{m}$  at the centre and expands to about 13  $\mu\text{m}$  towards each end. In addition, as seen in detail in Fig. 3(b), diopside crystals look like brooms embedded in the parent glass matrix. Further, their clustering suggests that they seem to have grown together in a bundle. Overall, the morphology, orientation and size of these crystals clearly indicate that surface crystallization took place in only one preferred orientation. According to Vekey *et al.*,<sup>8</sup> the effectiveness of bulk nucleation in the  $\text{CaO}$ - $\text{MgO}$ - $\text{Al}_2\text{O}_3$ - $\text{SiO}_2$  system can be enhanced by adding small amounts of alkaline oxides as diffusion accelerators. Although a total of 10% alkaline oxide and 10% titania nucleant was used in this study, these additions were still not sufficient to induce bulk crystallization within the parent glass matrix. This is believed to be due to using glass-forming raw materials instead of technical powders as the starting batch. Nevertheless, information regarding the surface crystallization can be used to determine the activation energy for crystallization. As stated by Matusita and Sakka,<sup>29</sup> it is necessary to examine and know the crystallization mechanism for analysing crystallization kinetics and obtaining a meaningful activation energy. In the following section, the graphical determination of the activation energy for diopside crystallization as a result of surface nucleation is presented.

### 3.3 Activation energy determination

The DTA curves shown in Fig. 1 can be used to determine the activation energy for crystal growth by analysing the exothermic peak heights on the basis of the nucleation and growth equations.<sup>25,26</sup> As stated by Sestak,<sup>30</sup> the activation energy term is a composite quantity contributed by nucleation, crystal growth and diffusion processes. Adopting the same assumption of Matusita and Sakka<sup>29</sup> that the number of crystal nuclei formed at temperatures above  $T_g$  is constant in a glass matrix, the rate of change of volume fraction of crystals can be defined as:

$$\frac{dx}{dt} = KB^{(n-1)}(1-x)^k \exp\left(-\frac{mQ}{RT}\right) \quad (1)$$

with its maximum at  $T = T_p$  for any non-isothermal DTA condition. Therefore, as stated by Matusita and Sakka,<sup>29</sup> eqn (1) can be solved at  $d/dt(dx/dt) = 0$  and re-expressed as:

$$\ln\left(\frac{B^n}{T_p^2}\right) = -\frac{mQ}{RT_p} + \text{constant} \quad (2)$$

assuming that the term  $(1 - x_c)^k$  is constant for  $x = x_c$ ,  $T = T_p$ . Thus it seems that the three unknowns in eqn (2) can be calculated using the parameters  $B$  and  $T_p$  given in Table 1 in five equations. However, this assumption only holds if the exact crystallization mechanism is determined and that employing different DTA heating rates does not alter it. On the basis of SEM characterization that crystallization takes place as a result of surface nucleation,  $n = m = 1$  for all heating rates can be assumed which leads to the Kissinger equation:<sup>25</sup>

$$\ln \left( \frac{B}{T_p^2} \right) = - \frac{Q}{RT_p} + \text{constant} \quad (3)$$

Figure 4 is a graphical solution of eqn (3) where the  $T_p$  and  $B$  values listed in Table 1 are used to plot  $\ln(B/T_p^2)$  as a function of  $1/T_p$  to calculate the activation energy for crystallization. As seen in Fig. 4, parameters measured in five different non-isothermal DTA analyses provide a linear fit of data points and the slope is nothing but  $Q/R$  (where  $R = 8.31 \text{ J/Kmole}$ , gas constant). As seen in Fig. 4, the activation energy,  $Q$  can then be calculated as  $150 \text{ kJ/mole}$ . The DTA analyses were also conducted on the same glass system without  $\text{TiO}_2$  and the activation energy for this case was found as  $310 \text{ kJ/mole}$ <sup>21,22</sup> which is twice that of the titania-containing system of the present study, as expected. Similarly, the activation energy value of the present investigation is half that reported by Baldi *et al.*<sup>20</sup> where diopside was the major crystallizing phase in the ternary  $\text{SiO}_2\text{-CaO-MgO}$  system. However, this is in agreement with the inference by Matusita and Sakka<sup>29</sup> that for a given glass-ceramic material, activation energy for surface crystallization is generally lower than that for bulk crystallization.

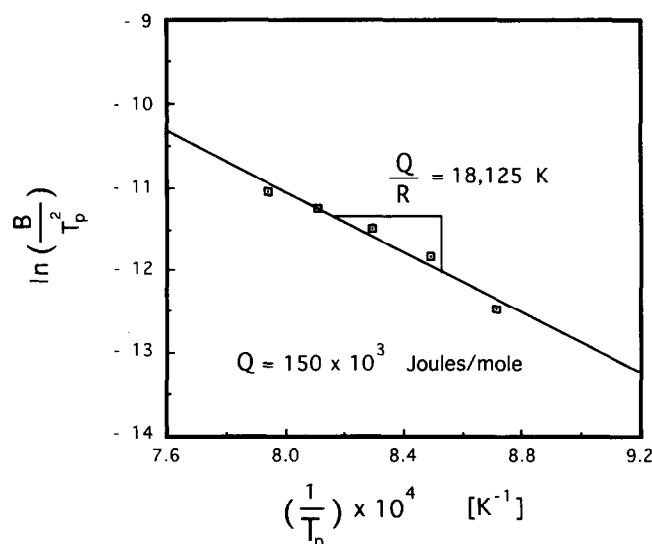


Fig. 4. Graphical determination of the activation energy for crystallization of the diopside-based glass-ceramic; Kissinger plot of data obtained from DTA curves shown in Fig. 1 and reported in Table 1.

## 4 Conclusions

This study has been an attempt to clearly show that glass industry raw materials can be utilized for the development and large scale production of glass-ceramic articles. Based on the results reported in the present investigation, the following conclusions can be drawn:

- (1) The addition of 10%  $\text{TiO}_2$  enables the devitrification of the investigated glassy system which results in the formation of the crystalline phase identified as diopside-aluminan  $\text{Ca}(\text{Mg}, \text{Al})(\text{Si}, \text{Al})_2\text{O}_6$ . Diopside is the only crystallizing phase comprising about 74 vol% in the parent glass matrix.
- (2) Since non-technical grade glass-forming raw materials are used in this study, diopside-aluminan crystals form as a result of surface nucleation and have a size range between 15 and  $40 \mu\text{m}$  whereas their widths vary between 5 and  $13 \mu\text{m}$ .
- (3) The peak crystallization temperatures and different non-isothermal heating rates determined by DTA analyses were used in the same equations derived by Matusita and Sakka and the activation energy for surface crystallization was calculated as  $150 \text{ kJ/mole}$  from the slope of the Kissinger plot. This value is half of that for the surface crystallization of the same glass composition without the nucleant content.

## Acknowledgments

The authors wish to thank the management of Şişecam (Turkish Bottle and Glassworks) Research Centre for providing necessary research facilities during the course of this study. One of the authors (M. L. Ö.) would like to thank his colleagues in the department of Metallurgical Engineering of Istanbul Technical University for useful discussions regarding this work.

## References

1. Stookey, S. D., US Patent No. 2,920,971, 12 January 1960.
2. McMillan, P. W., *Glass-Ceramics*. Academic Press, London, 1964.
3. Takehara, T., US Patent No. 3,170,780, 23 February 1965.
4. Leger, L. and Bray, J., An experimental study of the controlled crystallization of alkaline-earth silico-aluminate glasses. *J. Glass. Tech.*, 1996, 7(4), 134-142.
5. Williamson, J., Tipple, A. J. and Rogers, P. S., The effect of vanadium oxides on the crystallization of silicate glasses. *J. Mat. Sci.*, 1968, 4, 1069-1074.

6. Williamson, J., Tipple, A. J. and Rogers, P. S., Influence of iron oxides on kinetics of crystal growth in CaO–MgO–Al<sub>2</sub>O<sub>3</sub>–SiO<sub>2</sub>. *J. Iron and Steel Industry*, 1968, **206**, 898–903.
7. Davies, M. W., Kerrison, B., Gross, W. E., Robson, M. J. and Wichall, D. F., Slagceram: A glass-ceramic from blast-furnace slag. *J. Iron and Steel Industry*, 1970, **208**(4), 348–370.
8. De Vekey, R. C. and Majumdar, A. J., Nucleation and crystallization studies of some glasses in the CaO–MgO–Al<sub>2</sub>O<sub>3</sub>–SiO<sub>2</sub> system. *Min. Mag.*, 1970, **37**, 771–779.
9. Veasey, T. J., Recent developments in the production of glass-ceramics. *Mineral Science and Engineering*, 1973, **5**(2), 92–104.
10. De Vekey, R. C. and Majumdar, A. J., The effect of fabrication variables on the properties of cordierite-based glass-ceramics. Part 1. The effect of variables in heat treatment. *Glass Technology*, 1973, **14**(5), 125–134.
11. De Vekey, R. C. and Majumdar, A. J., The effect of fabrication variables on the properties of cordierite-based glass-ceramics. Part 2. The effect of composition. *Glass Technology*, 1974, **15**(3), 71–80.
12. De Vekey, R. C. and Majumdar, A. J., Metastable zoning cordierite-based glass-ceramics. *Mat. Res. Bull.*, 1973, **8**, 1073–1078.
13. De Vekey, R. C. and Majumdar, A. J., The role of TiO<sub>2</sub> in the formation of cordierite glass-ceramics. *Physics and Chemistry of Glasses*, 1975, **16**(2), 36–43.
14. Orsini, P. G., Buri, A. and Marotta, A., Devitrification of glasses in the akermanite-gehlenite system. *J. Am. Ceram. Soc.*, 1975, **58**(7-8), 306–311.
15. Zdaniewski, W., DTA and X-ray analysis study of nucleation and crystallization of CaO–MgO–Al<sub>2</sub>O<sub>3</sub>–SiO<sub>2</sub> glasses containing ZrO<sub>2</sub>, TiO<sub>2</sub> and CeO<sub>2</sub>. *J. Am. Ceram. Soc.*, 1975, **58**(5-6), 163–169.
16. Zdaniewski, W., Microstructure and kinetics of crystallization of MgO–Al<sub>2</sub>O<sub>3</sub>–SiO<sub>2</sub> glass-ceramic. *J. Am. Ceram. Soc.*, 1975, **61**(5-6), 199–204.
17. Karyakin, V. A. and Sazonov, A. A., Production of ash-based glass ceramic curbstone. *Nov. Tekhnol. Kamen. Lit'ya*, 1981, 91–100 [in Russian].
18. Kruchinin, Yu. D. and Karyakin, V. A., Conditions for synthesis of iron-containing pyroxene and spinel-pyroxene glass ceramics. *Izv. Akad. Nauk SSSR, Neorg. Mater.*, 1983, **19**(4), 665–669 [in Russian].
19. Ismatov, A. A., Tashmetova, O. A. and Abdullaev, Kh. A., Use of untreated secondary angren kaolins for production of glass-ceramics. *Uzb. Khim. Zh.*, 1984, **5**, 83–84 [in Russian].
20. Baldi, G., Generali, E., Leonelli, C., Manfredi, T., Pellacani, G. C. and Sligardi, C., Effects of nucleating agents on diopside crystallization in new glass-ceramics for tile-glaze application. *J. Mat. Sci.*, 1995, **30**, 3251–3255.
21. Kuban, B., Development of glass-ceramics from raw materials used in glass industry. Şişecam Research Center Final Report No. 331, 1992.
22. Çam, A., Investigation of kinetic factors via DTA techniques in a glass-ceramic containing different nucleants. Graduation Thesis, Istanbul Technical University, Istanbul, Turkey, June 1993.
23. Özer, H., Öveçoğlu, M. L. and Kuban, B., Microstructural and chemical properties of diopside-based glass-ceramics. In *2nd International Ceramics Congress-Istanbul*, 1994, Vol. 2, pp. 414–427.
24. Borchardt, H. J. and Daniels, F., The application of thermal analysis to the study of reaction kinetics. *J. Am. Ceram. Soc.*, 1957, **79**, 41–46.
25. Kissinger, H. E., Variation of peak temperature with heating rate in differential thermal analysis. *J. Res. Nat. Bur. Stand.*, 1956, **57**, 217–221.
26. Kissinger, H. E., Reaction kinetics in differential thermal analysis. *Anal. Chem.*, 1957, **29**, 1702–1706.
27. Thakur, R. L. and Thiagarajan, S., Studies in catalyzed crystallization of glasses: A DTA method. *Cent. Glass Ceram. Res. Inst. Bull.*, 1966, **13**, 33–45.
28. Skvára, F. and Satava, V., Kinetic data from DTA measurements. *J. Thermal Anal.*, 1970, **2**, 325–335.
29. Matusita, K. and Sakka, S., Kinetic study on crystallization of glass by differential thermal analysis — Criterion on application of Kissinger plot. *J. Non-cryst. Solids*, 1980, **38&39**, 741–746.
30. Sestak, J., The applicability of DTA to the study of crystallization kinetics of glasses. *Physics and Chemistry of Glasses*, 1974, **15**(6), 137–140.
31. *Powder Diffraction File*, Card no. 41-1370, 1992 Database Edition, Joint Committee on Powder Diffraction Standards, Swathmore, PA, USA.
32. *Powder Diffraction File*, Card no. 21-1276, 1992 Database Edition, Joint Committee on Powder Diffraction Standards, Swathmore, PA, USA.
33. Chung, F. H., Quantitative interpretation of X-ray diffraction patterns of mixtures. I. Matrix-flushing method for quantitative multicomponent analysis. *J. Appl. Cryst.*, 1974, **7**, 519–525.
34. Chung, F. H., Quantitative interpretation of X-ray diffraction patterns of mixtures. III. Simultaneous determination of a set of reference intensities. *J. Appl. Cryst.*, 1975, **8**, 17–19.
35. Ohlberg, S. M. and Strickler, D. W., Determination of percent crystallinity of partly devitrified glass by X-ray diffraction. *J. Am. Ceram. Soc.*, 1962, **45**(4), 170–171.